Nuclear Medicine and Biology 39 (2012) 770–776

Contents lists available at SciVerse ScienceDirect

Nuclear Medicine and Biology

journal homepage: www.elsevier.com/locate/nucmedbio

A preclinical investigation of the saturation and dosimetry of ^{153}Sm-DOTMP as a bone-seeking radiopharmaceutical☆

Jaime Simón [a,*], R. Keith Frank [a], Druce K. Crump [a], William D. Erwin [b], Naoto T. Ueno [c], Richard E. Wendt III [b]

[a] IsoTherapeutics Group, LLC, Angleton, TX 77515, USA
[b] Department of Imaging Physics, The University of Texas M. D. Anderson Cancer Center, Houston, Texas, USA
[c] Department of Breast Medical Oncology, The University of Texas M. D. Anderson Cancer Center, Houston, Texas, USA

ARTICLE INFO

Article history:
Received 30 September 2011
Received in revised 19 November 2011
Accepted 14 December 2011

Keywords:
^{153}Sm-DOTMP
Bone-seeking radiopharmaceutical
Preclinical study

ABSTRACT

Introduction: The therapeutic potential of the bone-seeking radiopharmaceutical 153Sm-labeled 1,4,7,10-tetraazacyclododecanetetramethylenephosphonic acid (153Sm-DOTMP) was assessed by measuring its dosage-dependent skeletal uptake at two chelant-to-metal ratios and its source organ residence times at a chelant-to-metal ratio of 1.5:1. A similar agent, 153Sm-labeled ethylenediaminetetramethylenephosphonic acid (153Sm-EDTMP), has been reported to exhibit dosage-limiting skeletal saturation.
Methods: Sm-DOTMP was prepared with tracer activity of 153Sm and sufficient stable, unenriched Sm to simulate different activities. Cohorts of seven 280-g Sprague–Dawley rats were administered the equivalent of 296, 592, 888, 1184 and 1480 MBq (8, 16, 24, 32 and 40 mCi) at a fixed chelant-to-metal ratio of 1.5:1 and euthanized 3 h after administration. Cohorts of three 128-g Sprague–Dawley rats were administered equivalent dosages of 10.4, 592 and 888 (0.28, 16 and 32 mCi) at a fixed chelant-to-metal ratio of 270:1 and euthanized 2 h after administration. A simulated activity of 1480 MBq (40 mCi) at a chelant-to-metal ratio of 1.5:1 was administered to cohorts of seven rats that were euthanized at 2, 4, 24 or 48 h postadministration. The heart, lungs, liver, spleen, kidneys, small intestine, large intestine, urinary bladder, muscle and a femur were excised, weighed and counted. The data were analyzed to determine skeletal uptake and source organ residence times.
Results: No statistically significant skeletal saturation was observed up to human-equivalent dosages of 370 GBq (10 Ci) at a chelant-to-metal ratio of 1.5:1, but the skeletal uptake dropped by 40% over the range of dosages at a chelant-to-metal ratio of 270:1. At a chelant-to-metal ratio of 1.5:1, the preferred ratio, the skeletal uptake fraction in rats was 0.408 (95% confidence interval 0.396–0.419) with an effective half-life of 47.3 h (95% confidence interval 42.3–53.7; the physical half-life of 153Sm is 46.3 h). Extrapolating to an adult human model, 52.9 GBq (1.43 Ci) of 153Sm-DOTMP would deliver 40 Gy to the red marrow.
Conclusion: 153Sm-DOTMP has dosimetry equivalent to that of 153Sm-EDTMP at low dosages, yet with no skeletal saturation at higher administered activities.

1. Introduction and background

So-called "bone-seeking" radiopharmaceuticals are attractive agents for the palliation of pain from bone metastases and for the treatment of bone tumors and ablation of the bone marrow [1]. ^{153}Sm-labeled 1,4,7,10-tetraazacyclododecanetetramethylenephosphonic acid (^{153}Sm-DOTMP) is a radiopharmaceutical that combines a chelant that is readily taken up by growing bone with a radionuclide that has a half-life of 46.3 h and that emits both gamma rays and beta particles.

The studies reported here had two objectives. The first was to assess in a rat model whether or not ^{153}Sm-DOTMP is subject to the saturation effect that has been reported for a similar compound, ^{153}Sm-labeled ethylenediaminetetramethylenephosphonic acid (^{153}Sm-EDTMP), at high dosages [2–4]. The second was to measure the biodistribution and kinetics of ^{153}Sm-DOTMP in a rat model and to extrapolate those measurements to human beings in order to estimate human target organ doses.

^{153}Sm-DOTMP has previously been investigated by Simón et al. [5–7], Chakraborty et al. [8], Banerjee et al. [9] and Chiotellis et al. [10]. Their preclinical results demonstrated skeletal uptake fractions of 0.69, 0.60 and 0.39, respectively, with good long-term retention. While these earlier data suggest that ^{153}Sm-DOTMP has promise as a bone-seeking radiopharmaceutical, it has not yet been investigated in

☆ Supported by the National Cancer Institute R43CA150601.
* Corresponding author. Tel.: +1 979 848 0800; fax: +1 979 848 0807.
E-mail address: jimsimon@isotherapeutics.com (J. Simón).

0969-8051/$ – see front matter © 2012 Elsevier Inc. All rights reserved.
doi:10.1016/j.nucmedbio.2011.12.015

human clinical trials for bone pain palliation, treatment of bone lesions or bone marrow ablation with curative intent.

Bartlett et al. [2] advanced the hypothesis that the saturation effect that they had observed in high-dose ^{153}Sm-EDTMP therapy arises from a saturation of the skeletal uptake sites with EDTMP molecules. Such saturation has been observed in studies in vitro [11]. Bartlett et al. noted the high chelant-to-metal ratio of ^{153}Sm-EDTMP (273:1 in the US formulation) and proposed that this ratio might be reduced in order to lessen the saturation effect. That is not feasible in practice. The high chelant-to-metal ratio of ^{153}Sm-EDTMP is necessary in order to keep the ^{153}Sm bound and thus to prevent undesired uptake of ^{153}Sm in the liver [12,13]. Typically, the specific activity of ^{153}Sm is low (about 2% of the theoretical maximum based on the neutron flux at the University of Missouri Research Reactor). While higher-specific-activity ^{153}Sm would partially address this issue, it is presently not available. Consequently, a better chelant than EDTMP is needed in order to reduce the chelant-to-metal ratio and hence the total amount of chelant administered and thereby to avoid the postulated saturation effect. This observation prompted us to reconsider ^{153}Sm-DOTMP because DOTMP binds ^{153}Sm tightly with chelant-to-metal ratios as low as 1.5:1 [5]. The studies that are reported here evaluated the potential of ^{153}Sm-DOTMP to deliver ^{153}Sm to the skeletal surfaces at significantly higher administered activities than appear to be practical with ^{153}Sm-EDTMP.

2. Materials and methods

The ligand DOTMP was synthesized by reacting cyclam (1,4,7,11 tetraazadodecane) with phosphorous acid and formaldehyde in hydrochloric acid under reflux conditions. Purification was accomplished by multiple recrystalizations. Structure confirmation was done by nuclear magnetic resonance, and the product showed a single peak on ion exchange high-performance liquid chromatography.

^{153}Sm was obtained from the University of Missouri Research Reactor at a specific activity of 13.25 TBq/g or 2030 TBq/mol (358 Ci/g or 54,700 Ci/mol) at the time of shipment.

Sm-DOTMP was prepared by mixing the appropriate amount of aqueous ligand and metal in a vial in acidic solution. The pH of the solution was adjusted to a value between 9 and 9.5 using NaOH. A sample of the solution was analyzed for free metal using a gravity cation exchange column. The pH was then adjusted to a value between 7 and 8 using phosphate buffer, and the solution was again analyzed for free metal by ion exchange. In all cases, less than 0.1% of the activity was found as free metal. Thus, all chelates administered were greater than 99% Sm-DOTMP.

For the first study, dosages of ^{153}Sm-DOTMP were prepared with a nominal activity of 370 kBq (10 μCi) of ^{153}Sm (377±25.9 kBq or 10.2 ±0.7 μCi) and with sufficient stable, unenriched Sm to simulate activities of 296, 592, 888, 1184 and 1480 MBq (8, 16, 24, 32 and 40 mCi) of ^{153}Sm-DOTMP at a chelant-to-metal ratio of 1.5:1 as shown in Table 1. A similar procedure was used to prepare dosages with simulated activities of 10.4, 592 and 1184 MBq (0.28, 16 and 32 mCi) at a chelant-to-metal ratio of 270:1 for the second study.

The total mass of Sm that is required to simulate a particular activity is the simulated activity divided by the specific activity of the ^{153}Sm stock preparation at the time for which the activity is calibrated. The mass of stock ^{153}Sm that is required in order to produce the actually administered activity (370 kBq in this study) is the activity actually to be administered divided by the specific activity. The difference in these two masses is the mass of stable Sm that must be added to the actually administered activity in order to simulate the desired activity. For example, to simulate a 296-MBq (8-mCi) administered activity using stock ^{153}Sm with the above-given specific activity, one would need 20.779 μg of the stock ^{153}Sm at that specific activity. For an actually administered activity of 370 kBq (10 μCi), yet with a simulated activity of 296 MBq (8 mCi), one would use only 2.597×10^{-2} μg of the stock ^{153}Sm with stable Sms constituting the remainder of the 20.779-μg mass, i.e., 20.753 μg.

The injected volume was nominally 100 μl (96.4±6.4 μl) for the first study and 200 μl (198.1±1.9 μl) for the second study.

For the second study, the three cohorts received simulated activities of 10.4, 592 and 1184 MBq (0.28, 16 and 32 mCi) that were prepared with actual activities of 488±3.7, 545±2.1 and 798 ±5.7 kBq (13.2±0.1, 14.7±0.1 and 21.6±0.2 μCi), respectively. For the third study, the 1480-MBq (40-mCi) activity was simulated with an actual administered activity of 396±22.2 kBq (10.7±0.6 μCi) in a volume of 99.0±2.4 μl.

The first and third studies were performed using male Sprague–Dawley rats with a nominal weight of 280 g (first study: 275.1±11.1 g; third study: 271.5±9.7 g). The second study used male Sprague–Dawley rats with a nominal weight of 128 g (128.0±3.1 g). These studies were reviewed and approved by the Animal Care and Use Committee of IsoTherapeutics Group, LLC, and conducted in compliance with the relevant laws regulating this animal research.

Each cohort in the first and third studies consisted of seven rats. Each cohort in the second study contained three animals. The rats were fed a standard diet (2014 Rodent Feed, Harlon Laboratories, Indianapolis, IN, USA) and water ad lib both before and after administration.

The radiopharmaceutical was injected into the tail vein of the rats using a 28-gauge needle. A warm water bath and a heat lamp were used to dilate the vessel. Following administration, the rats were placed in individual cages so that all excreta could be collected and counted. After a circulation time detailed below, each animal was rendered unconscious by inhalation anesthesia (5% isoflurane) and killed by cervical dislocation.

The heart, lungs, liver, spleen, kidneys, small intestine, large intestine, urinary bladder, a femur and the muscles surrounding the femur were dissected, placed in previously weighed counting tubes and weighed. The cages were rinsed with a chelating solution (Scrubbing Bubbles, SC Johnson, Racine, WI, USA) that was then added to the counting tube that contained the bladder along with any urine spots on the absorbent paper covering the dissection surface to give an estimate of the activity excreted by the animal.

Each of these tubes was counted, along with a standard, for 1 min using the preset ^{153}Sm window on a sodium iodide well counter (103 keV center; width automatically set to incorporate 93% of the counts in the wide-window spectrum; Wizard 1480, Perkin-Elmer Life Sciences, Boston, MA, USA).

Table 1
Preparation of the simulated activities of Sm-DOTMP that were administered to rats in the first and third studies.

Human administered activity (GBq; Ci)	Equivalent activity to be simulated in rat (MBq; mCi)	Total Sm needed (mg; mmol)	^{153}Sm needed (mg; mmol)	Stable Sm needed (mg; mmol)
74; 2	296; 8	20.779×10^{-3}; 1.3588×10^{-4}	2.597×10^{-5}; 1.6982×10^{-7}	20.753×10^{-3}; 1.3571×10^{-4}
148; 4	592; 16	41.558×10^{-3}; 2.7176×10^{-4}	2.597×10^{-5}; 1.6982×10^{-7}	41.532×10^{-3}; 2.7159×10^{-4}
232; 6	888; 24	62.338×10^{-3}; 4.0765×10^{-4}	2.597×10^{-5}; 1.6982×10^{-7}	62.312×10^{-3}; 4.0748×10^{-4}
296; 8	1184; 32	83.117×10^{-3}; 5.4353×10^{-4}	2.597×10^{-5}; 1.6982×10^{-7}	83.091×10^{-2}; 5.4336×10^{-3}
370; 10	1480; 40	103.896×10^{-3}; 6.7940×10^{-4}	2.597×10^{-5}; 1.6982×10^{-7}	103.87×10^{-2}; 6.7923×10^{-3}

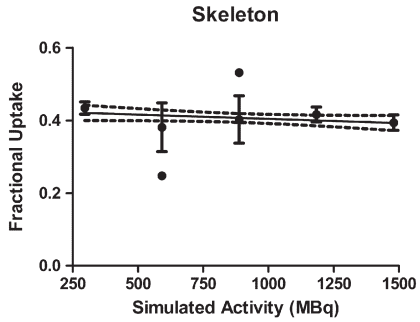

Fig. 1. Skeletal uptake as a function of simulated activity at 3 h after administration. The two isolated circles represent data points that were excluded from the analysis as outliers. The error bars are the 95% confidence intervals for the data points, and the dashed lines represent the 95% confidence intervals of the linear fit to the data.

The count data were compared to counts in the standard to obtain the fraction of the radioactivity in organs and tissues. Since all samples were counted within minutes of counting the standard, the data were effectively decay corrected. The data were recorded as the percentage of the injected dosage (%ID) per unit mass, %ID/g, except for the excreta. For organs that were dissected in whole, the %ID/g was multiplied by the measured mass of the tissue to get %ID. To minimize small errors associated with weighing milligram quantities of the standards, the %ID values were corrected for total recovery of the radionuclide in each animal.

To estimate the skeletal mass of the rats, Table 53 in the work of Donaldson [14] relating moist skeleton weight (SW) to total body weight (TBW) was fit by the equation SW=0.0458×TBW−3.4028 with all masses in grams. This fit has R^2=0.9639 over a range of total body weight from 77 to 460 g. To estimate the muscle mass of the rats, Donaldson's Chart 5 showing the fraction of total body weight that is muscle as a function of age and Eq. (35) relating total body weight to age were combined, and muscle mass (MM) as a fraction of total body weight was fit by the equation MM=0.5079×TBW−17.737 with all masses in grams. This fit has R^2=0.9941 over the range of total body weight from 166 to 280 g. The %ID/g values of the dissected portions of bone and muscle were assumed to be representative of the tissues as a whole, and those %ID/g values were multiplied by the total tissue masses estimated from these equations to estimate the %ID for bone and for muscle.

In the saturation studies, the data for each tissue were plotted against the simulated administered activity and fit by a linear regression (Prism, GraphPad Software, La Jolla, CA, USA). Examples are shown in Figs. 1 and 2. In the distribution study, the data for each tissue were plotted against the length of time between administration and sacrifice and were fit by a single exponential function, a double exponential function or a collection of trapezoids of which representative curves are shown in Fig. 3.

For the first saturation study, five cohorts of animals were administered simulated activities of 296, 592, 888, 1184 and 1480 MBq (8, 16, 24, 32 or 40 mCi) of Sm-DOTMP at a chelant-to-metal ratio of 1.5:1 and euthanized 3 h after administration. The actual radioactivity was nominally 370 kBq (10 μCi) in all cases. Three data points were excluded from the fits as outliers using the automated outlier detection of the statistical software based upon the default Q parameter of 1%. For the second saturation study, three cohorts of three animals each were administered simulated activities of 10.4, 592 and 1184 MBq (0.28, 16 and 32 mCi) of Sm-DOTMP at a chelant-to-metal ratio of 270:1 and euthanized 2 h after administration.

For the distribution study, four cohorts of animals were administered a simulated activity of 1480 MBq (40 mCi) of Sm-DOTMP at a chelant-to-metal ratio of 1.5:1 and euthanized at 2, 4, 24 or 48 h after administration. The simulated activity level for the distribution study was chosen after the analysis of the first saturation study had demonstrated no measurable saturation effect at even the highest dosage with a chelant-to-metal ratio of 1.5:1. The 3-h, 40-mCi data from the first saturation study were also included as a time point in the distribution data. These decay-corrected data were decayed by the physical half-life of ^{153}Sm, 46.3 h, before analysis and curve fitting in order to estimate the source organ residence times.

The residence times were calculated from the exponential terms using the equation $T_{res}=1.443\times A_0 T_{eff0}+1.443\times A_1 T_{eff1}$ where A_i is the fractional uptake for the ith component, T_{effi} is the effective half-life for the ith component and $A_1=0$ for single exponential fits. The area

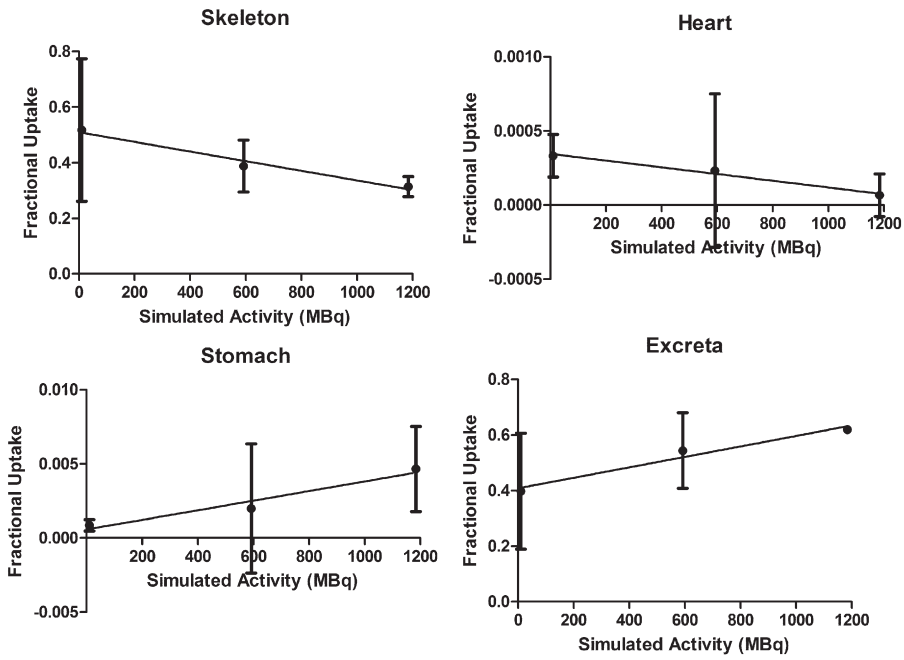

Fig. 2. Uptake as a function of simulated activity for the four tissues that had significantly nonzero slopes. The error bars are the 95% confidence intervals for the data points.

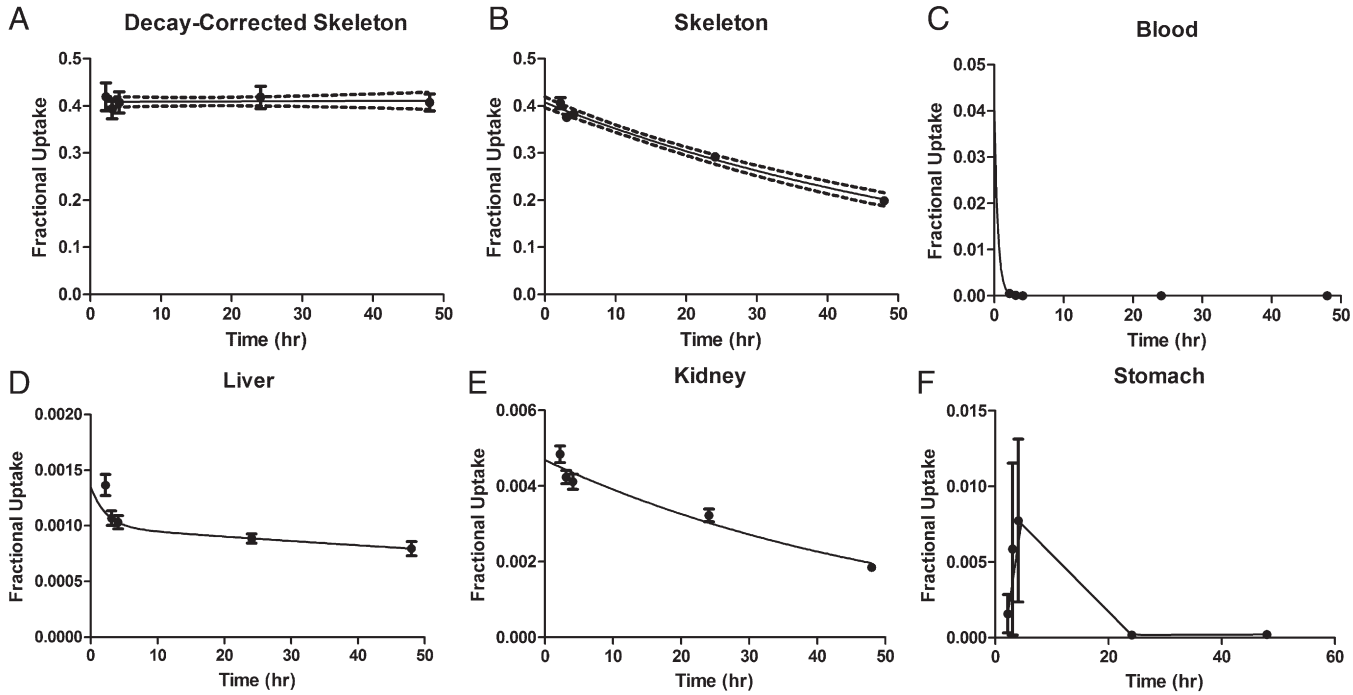

Fig. 3. (A) Decay-corrected time–activity curve for the skeleton. The 95% confidence intervals are indicated by the dashed lines. (B–F) Representative time–activity curves including physical decay of the skeleton, blood, liver, kidneys and stomach, respectively. The vertical axes are the fraction.

under the curve equals the residence time for the data fit by trapezoids because the later data points were nil for these tissues. The skeletal residence time was apportioned as 62% to the trabecular bone and 38% to the cortical bone. The source organ residence times were entered into the OLINDA/EXM [15] 1.1 software (Vanderbilt University, Nashville, TN, USA) to calculate target organ doses for the 73.7-kg adult male model.

3. Results

3.1. Saturation

The straight line fits of the tissue fractional uptake data as a function of simulated dosage activity are summarized in Tables 2 and 3.

No tissue had a significantly nonzero slope (i.e., a statistically significant dependence of uptake upon simulated activity) using $P<.05$ as the criterion for significance with a chelant-to-metal ratio of 1.5:1.

For the chelant-to-metal ratio of 270:1, the slope of the fractional uptake as a function of simulated activity was significantly nonzero for the skeleton ($P=.0048$), the heart ($P=.0303$), the stomach ($P=.0059$) and the excreta ($P=.0021$). Plots of these data are shown in Fig. 2. The other tissues had slopes that were not significantly different from zero at the level of $P<.05$.

3.2. Distribution

The analysis of the tissue fractional uptake data as a function of time following administration is summarized in Table 4. Values only for A_0 and T_{eff0} imply a single exponential fit; values for A_0, A_1, T_{eff0} and T_{eff1} imply a double exponential fit; and a value for AUC implies that the data points were fit by trapezoids making a closed figure that returned to zero at the 24-h time point and that the area under the trapezoids was then determined. The slope of the linear regression of the time–activity curve of the decay-corrected excreta was not significantly nonzero ($P=.0690$).

Table 2
Fit data for the tissue uptakes as a function of simulated dosage (in MBq) for the first saturation study, which had a chelant-to-metal ratio of 1.5:1.

Organ	Slope	Y-intercept	Slope P	Excluded outliers
Blood	$-5.01\times10^{-7}\pm4.36\times10^{-7}$ [-1.39×10^{-6}, 3.86×10^{-7}]	$8.00\times10^{-4}\pm4.28\times10^{-4}$ [-7.14×10^{-5}, 1.67×10^{-3}]	.258	0
Bone	$-2.34\times10^{-5}\pm1.40\times10^{-5}$ [-5.20×10^{-5}, 5.20×10^{-6}]	0.428±0.0139 [0.399, 0.456]	.105	2
Heart	$1.26\times10^{-8}\pm1.52\times10^{-8}$ [-1.84×10^{-8}, 4.35×10^{-8}]	$2.06\times10^{-5}\pm1.49\times10^{-5}$ [-9.80×10^{-6}, 5.09×10^{-5}]	.415	0
Kidneys	$3.28\times10^{-7}\pm3.44\times10^{-7}$ [-3.73×10^{-7}, 1.03×10^{-6}]	$4.18\times10^{-3}\pm3.38\times10^{-4}$ [3.49×10^{-3}, 4.87×10^{-3}]	.348	0
Large intestine	$3.09\times10^{-6}\pm7.61\times10^{-6}$ [-1.24×10^{-5}, 1.86×10^{-5}]	$7.54\times10^{-3}\pm7.47\times10^{-3}$ [-7.66×10^{-3}, 2.27×10^{-2}]	.688	0
Liver	$-2.06\times10^{-7}\pm5.99\times10^{-7}$ [-1.43×10^{-6}, 1.01×10^{-6}]	$1.64\times10^{-3}\pm5.88\times10^{-4}$ [4.38×10^{-4}, 2.83×10^{-3}]	.733	0
Lungs	2.90×10−8±4.25×10−8 [−5.76×10−8, 1.16×10^{-7}]	$1.47\times10^{-4}\pm4.18\times10^{-5}$ [6.16×10^{-5}, 2.32×10^{-4}]	.501	0
Muscle	$-1.22\times10^{-5}\pm6.32\times10^{-6}$ [-2.51×10^{-5}, 6.93×10^{-7}]	$2.39\times10^{-2}\pm6.26\times10^{-3}$ [1.12×10^{-2}, 3.67×10^{-2}]	.063	1
Small intestine	$6.68\times10^{-6}\pm9.34\times10^{-6}$ [-1.23×10^{-5}, 2.57×10^{-5}]	$4.54\times10^{-3}\pm9.17\times10^{-3}$ [-1.41×10^{-2}, 2.32×10^{-2}]	.480	0
Stomach	$3.18\times10^{-6}\pm2.84\times10^{-6}$ [-2.60×10^{-6}, 8.96×10^{-6}]	$-6.46\times10^{-4}\pm2.79\times10^{-3}$ [-6.32×10^{-3}, 5.03×10^{-3}]	.271	0
Spleen	−3.67×10−8±8.52×10−8 [-1.37×10^{-7}, 2.10×10^{-7}]	$-7.06\times10^{-5}\pm8.37\times10^{-5}$ [-9.98×10^{-5}, 2.41×10^{-4}]	.670	0
Excreta	$-2.02\times10^{-5}\pm2.93\times10^{-5}$ [-3.94×10^{-5}, 7.98×10^{-5}]	0.502±0.0288 [0.443, 0.560]	.495	0

The format of the data is $M\pm$S.D. [−CI, +CI], where M is the arithmetic mean of the measurements, S.D. is their sample standard deviation, −CI is the lower limit of the 95% confidence interval of the mean and +CI is the upper limit of the 95% confidence interval of the mean. The column labeled "Slope P" is the likelihood that the observed data could have come from a truly horizontal line (i.e., that the uptake has no dependence at all upon the simulated activity) purely by chance.

Table 3
Fit data for the tissue uptakes as a function of simulated dosage (in MBq) for the second saturation study, which had a chelant-to-metal ratio of 270:1.

Organ	Slope	*Y*-intercept	Slope *P*
Blood	$-2.12\times10^{-7}\pm1.59\times10^{-6}$ [-3.97×10^{-6}, 3.55×10^{-6}]	$2.53\times10^{-3}\pm1.21\times10^{-3}$ [-3.46×10^{-4}, 5.40×10^{-3}]	.898
Bone	$-1.73\times10^{-4}\pm4.26\times10^{-5}$ [-2.74×10^{-4}, -7.25×10^{-5}]	0.511 ± 0.0326 [0.433, 0.587]	.0048
Heart	$-2.27\times10^{-7}\pm8.40\times10^{-8}$ [-4.26×10^{-7}, -2.87×10^{-8}]	$3.46\times10^{-4}\pm6.42\times10^{-5}$ [1.95×10^{-4}, 4.98×10^{-4}]	.0303
Kidneys	$1.33\times10^{-6}\pm7.38\times10^{-7}$ [-4.13×10^{-7}, 3.08×10^{-6}]	$3.05\times10^{-3}\pm5.64\times10^{-4}$ [1.72×10^{-3}, 4.38×10^{-3}]	.114
Large intestine	$-2.07\times10^{-7}\pm1.84\times10^{-6}$ [-4.57×10^{-6}, 4.16×10^{-6}]	$3.24\times10^{-3}\pm1.41\times10^{-3}$ [-8.80×10^{-5}, 6.58×10^{-3}]	.914
Liver	$4.25\times10^{-6}\pm2.06\times10^{-6}$ [-6.23×10^{-7}, 9.11×10^{-6}]	$3.84\times10^{-4}\pm1.57\times10^{-3}$ [-3.34×10^{-3}, 4.10×10^{-3}]	.0781
Lungs	$-1.71\times10^{-7}\pm9.91\times10^{-8}$ [-4.05×10^{-7}, 6.39×10^{-8}]	$4.46\times10^{-4}\pm7.58\times10^{-5}$ [2.67×10^{-4}, 6.25×10^{-4}]	.129
Muscle	$-1.75\times10^{-5}\pm1.35\times10^{-5}$ [-4.95×10^{-5}, 1.44×10^{-5}]	$3.28\times10^{-2}\pm1.03\times10^{-2}$ [8.40×10^{-3}, 5.72×10^{-2}]	.235
Small intestine	$2.79\times10^{-6}\pm2.05\times10^{-6}$ [-2.06×10^{-6}, 7.63×10^{-6}]	$1.28\times10^{-3}\pm1.56\times10^{-3}$ [-2.42×10^{-3}, 4.99×10^{-3}]	.216
Stomach	$3.24\times10^{-6}\pm8.32\times10^{-7}$ [1.27×10^{-6}, 5.21×10^{-6}]	$5.81\times10^{-4}\pm6.36\times10^{-6}$ [-9.24×10^{-4}, 2.08×10^{-3}]	.0059
Spleen	$2.00\times10^{-7}\pm2.00\times10^{-7}$ [-2.72×10^{-7}, 6.73×10^{-7}]	$2.81\times10^{-4}\pm1.53\times10^{-4}$ [-8.03×10^{-5}, 6.42×10^{-4}]	.350
Excreta	$1.88\times10^{-4}\pm3.97\times10^{-5}$ [9.44×10^{-5}, 2.82×10^{-4}]	0.409 ± 0.0303 [0.337, 0.481]	.0021

The format of the data is $M\pm$S.D. [−CI, +CI], where M is the arithmetic mean of the measurements, S.D. is their sample standard deviation, −CI is the lower limit of the 95% confidence interval of the mean and +CI is the upper limit of the 95% confidence interval of the mean. The column labeled "Slope *P*" is the likelihood that the observed data could have come from a truly horizontal line (i.e., that the uptake has no dependence at all upon the simulated activity) purely by chance. No data were excluded as outliers.

3.3. Estimated human dosimetry

Table 5 gives the source organ residence times for the rat, the organ masses for a 280-g rat and for a 73-kg adult human being and the estimated human residence time using the method of scaling by relative organ mass in the two species [17].

The dynamic bladder model was used with a fraction of 0.5925 (i.e., all but the skeletal fraction); an estimated half-life of 0.5 h based upon the fact that the slope of the excreta was not significantly nonzero, implying that the vast majority of the excreted activity had been eliminated by the 2-h time point; and a 4-h voiding interval to estimate a residence time in the urinary bladder of 1.89 h. The organ masses for the rat came from the Donaldson reference [14] if they were given or, for the intestines and the stomach, the average organ masses of the rats in these experiments.

Table 6 gives the human target organ doses that are estimated by applying the residence times in the human column of Table 5 to the adult male model in OLINDA/EXM 1.1 [15].

4. Discussion

This study was performed with tracer activities in order that all samples would have activity levels compatible with the counting instruments that were used. It thus excludes effects on the tissue uptake that might arise from differences in radiation absorbed dose had the full activities that were simulated actually been administered.

The desired radiation absorbed dose to the red marrow in previous high-dose trials of 166Ho-DOTMP for the treatment of multiple myeloma was 40 Gy [18]. We converted the residence times from ^{166}Ho to ^{153}Sm by applying the physical decay of ^{153}Sm to the decay-corrected time–activity curve data that had originally been measured with ^{166}Ho. We calculated that an administered activity of 196 GBq (5.3 Ci) of ^{153}Sm-DOTMP would be needed to deliver 40 Gy to the red marrow of a 70-kg adult. This dosage was scaled to the rat by the ratio of total body masses (0.280/70) to obtain an equivalent murine dosage of 784 MBq (21.2 mCi). We chose a set of simulated dosages in the rat (296, 592, 888, 1184 and 1480 MBq or 8, 16, 24, 32 and 40 mCi) that would have human equivalents that would span this anticipated dosage in human beings. It should be noted that 196 GBq is well beyond the 25-GBq point at which Bartlett et al. observed the onset of a saturation effect in their high-dose ^{153}Sm-EDTMP study [2].

The skeletal uptake fraction measured in rats in this study, 0.408, is less than that reported in two previous studies. The Simón reports of skeletal uptake fractions around 0.69 were based upon a total skeletal mass of 25 g in the conversion from fractional uptake per gram in a bone sample to total skeletal fractional uptake. That same conversion factor applied to the present data would give a skeletal uptake fraction of 0.63. The Banerjee results [9] were based upon experiments using rats that weighed between 200 and 300 g. Given the change in the rate of bone metabolism as animals mature, it is possible that the higher skeletal uptake fraction from the Banerjee data, 0.60, is a consequence of the authors having studied younger rats that had a higher rate of skeletal growth than would be expected in the older rats used in the first and third part of the present study. This hypothesis is consistent with the higher uptake fraction of 0.51 in our second saturation study, which used younger, 128-g rats. The skeletal uptake measured in the present biodistribution study agrees well with that of Chiotellis et al. [10].

4.1. Saturation

At a chelant-to-metal ratio of 270:1, an appreciable reduction in the skeletal uptake was observed. This is consistent with the clinical observations of Bartlett et al. for ^{153}Sm-EDTMP [2].

Table 4
Fit parameters for the organ uptakes as a function of the time between administration and sacrifice

Organ	A_0	T_{eff0} (h)	A_1	T_{eff1} (h)	AUC
Bone	0.408	47.3			
Blood	0.0401	0.348			
Heart	6.78×10^{-5}	3.74			
Lung	3.54×10^{-4}	1.41	0.000123	21.3	
Muscle	0.0759	0.818			
Liver	0.0003611	1.58	0.000990	152	
Spleen	7.42×10^{-5}	4.58	3.38×10^{-5}	55.0	
Kidney	0.00469	38.2			
Small intestine					0.301
Large intestine					0.564
Stomach					0.0911

A_0 and A_1 are activities normalized by the administered activity.

Table 5
Residence times (T_{res}) measured in rats and extrapolated to human beings

Organ	Rat		Human	
	T_{res} (h)	Organ mass (g)	Organ mass[16] (g)	T_{res} (h)
Total body		280	73,000	
Bone	27.8	16.2	5500	36.2
Blood	0.0202	16.2	5600	0.0267
Heart	0.000366	1.05	330	0.000441
Lung	0.00451	1.6	500	0.00541
Muscle	0.0895	124	29,000	0.0800
Liver	0.219	13	1800	0.1160
Spleen	0.00317	0.74	150	0.00246
Kidney	0.259	2.3	310	0.134
Small intestine	0.301	8.31	1000	0.139
Large intestine	0.564	9.60	670	0.151
Stomach	0.0911	3.68	400	0.0379

Table 6
Target organ doses for the adult male model in OLINDA/EXM 1.1

Target organ	Dose (mSv/MBq)	Dose (rem/mCi)
Adrenals	0.00736	0.0272
Brain	0.00885	0.0328
Breasts	0.00207	0.00766
Gallbladder wall	0.00304	0.0112
Lower large intestine wall	0.0485	0.179
Small intestine	0.0304	0.113
Stomach wall	0.0141	0.0522
Upper large intestine wall	0.0297	0.110
Heart wall	0.00373	0.0138
Kidneys	0.0751	0.278
Liver	0.0130	0.0482
Lungs	0.00551	0.0204
Muscle	0.00587	0.0217
Ovaries	0.00680	0.0252
Pancreas	0.00419	0.0155
Red marrow	0.755	2.79
Osteogenic cells	3.93	14.6
Skin	0.00314	0.0116
Spleen	0.00547	0.0202
Testes	0.00339	0.0125
Thymus	0.00304	0.0113
Thyroid	0.00483	0.0179
Urinary bladder wall	0.721	2.67
Uterus	0.00856	0.0317
Total body	0.0878	0.325
Effective dose equivalent	0.266	0.983
Effective dose	0.177	0.657

However, the saturation study did not detect a dosage-dependent variation in the skeletal uptake of ^{153}Sm-DOTMP at a chelant-to-metal ratio of 1.5:1. At a significance level of .05, none of the tissues had a slope to the linear fit of the uptake as a function of simulated activity that differed significantly from zero. Taking the lower 95% confidence limit for the slope, the difference in skeletal uptake fraction between a 370-MBq (10 mCi) and a 1480-MBq (40 mCi) simulated activity would be 0.06, dropping from 0.41 at 370 MBq (10 mCi) to 0.35 at 1480 MBq (40 mCi). While this extreme and unlikely situation for ^{153}Sm-DOTMP is appreciable, it is not nearly so pronounced an effect as is the apparent saturation effect of ^{153}Sm-EDTMP that is illustrated in Bartlett's Fig. 3 [2]. Bartlett et al. note the potentially dire consequence of this saturation effect on the dose to the urinary system. If dosages of ^{153}Sm-EDTMP were to be increased above 30 GBq, an increasing fraction of the administered activity would be excreted. Once the skeleton is saturated, further administered activity goes entirely to the urinary system. This is demonstrated in the plot of the fraction of the administered activity in the excreta as a function of simulated activity in Fig. 2. That extra excreted radioactivity does not increase the dose to the target organs but does increase the dose to the urinary system.

4.2. Residence times

The validity of the relative mass method [17] of conversion between species of the skeletal residence time is tenuous. Ideally, the relative bone surface areas of the two species should be used because ^{153}Sm-DOTMP is taken up on the surfaces of the bone. However, we have not found bone surface area data for the rat. We thus have had to assume that the bone surface area per unit of skeletal mass is the same for both species and then to convert between species using the relative mass method.

4.3. Dosimetry

The human dose estimates extrapolated from these rat data indicate that the osteogenic cells would receive a radiation absorbed dose from ^{153}Sm-DOTMP that is more than five times that of any other target organ. The dose to the urinary bladder wall, which is dependent in part upon the parameters chosen for the dynamic bladder model, is very close to that of the red marrow.

To deliver 40 Gy to the red marrow would require an administered activity of 53 GBq (1.43 Ci) of ^{153}Sm-DOTMP. This is appreciably less than the 196 GBq (5.3 Ci) dosage estimate upon which the first saturation study was based. The difference is due to the relatively low skeletal uptake fraction (as low as 0.15) of bone-seeking radiopharmaceuticals in multiple myeloma in the study from which the 196-GBq (5.3-Ci) figure was derived as compared to the 0.408 fractional uptake observed in this rat study. It is noteworthy that both of these administered activities are beyond the start of apparent saturation at 25 GBq in the study by Bartlett et al. [2] but that either seems to be feasible without saturation using ^{153}Sm-DOTMP at a chelant-to-metal ratio of 1.5:1.

The dose to the red marrow estimated here, 0.755 mSv/MBq, for ^{153}Sm-DOTMP is similar to the 0.78 mSv/MBq measured by Bartlett et al. [2] for ^{153}Sm-EDTMP. Using the residence times of Eary et al. [19] for ^{153}Sm-EDTMP as inputs to OLINDA/EXM 1.1 gives an estimate of the dose to the red marrow of 0.869 mSv/MBq for ^{153}Sm-EDTMP. This is reasonably close to the estimate from the present work for ^{153}Sm-DOTMP and to the measurement by Bartlett for ^{153}Sm-EDTMP.

5. Conclusion

^{153}Sm-DOTMP has very similar dosimetry to that of ^{153}Sm-EDTMP at low dosages. ^{153}Sm-DOTMP appears to overcome the saturation effect that has been observed in high-dose therapy with ^{153}Sm-EDTMP. The preclinical results reported here suggest that ^{153}Sm-DOTMP may be administered at dosages that would enable therapy with curative intent without the incommensurate elevation of the dose to the urinary system arising from the saturation effect of ^{153}Sm-EDTMP.

Acknowledgments

The authors gratefully acknowledge the support of the National Cancer Institute, R43CA150601. They thank Alan Ketring, Ph.D., for helpful discussions; Jason Rogers, Shannon Phillips, Ph.D., and Scot Ellebracht for expert technical assistance; Prakash Bakhru, M.S., for invaluable organizational support and practical advice and an anonymous reviewer for suggesting the saturation study at a 270:1 chelant-to-metal ratio.

References

[1] Friedell HL, Storaasli JP. The use of radioactive phosphorus in the treatment of carcinoma of the breast with widespread metastases to bone. Am J Roentgenol 1950;64:559–75.
[2] Bartlett ML, Webb M, Durrant S, Morton AJ, Allison R, Macfarlane DJ. Dosimetry and toxicity of Quadramet for bone marrow ablation in multiple myeloma and other haematological malignancies. Eur J Nucl Med 2002;29:1470–7.
[3] Erwin W, Mikell J, Ueno N. Predictive value of a pre-therapy tracer study skeletal retention estimate in high-dose Sm-153-EDTMP radiotherapy of skeletal metastatic breast cancer. J Nucl Med 2010;51:1143.
[4] van Rensburg AJ, Alberts AS, Louw WKA. Quantifying the radiation dosage to individual skeletal lesions treated with samarium-153-EDTMP. J Nucl Med 1998;39:2110–5.
[5] Simon J, Garlich JR, Wilson DA, McMillan K. Bone marrow suppressing agents, U.S. Patent 4,882 1989:142.
[6] Simon J, Wilson DA, Garlich JR, Troutner DE. Macrocyclic aminophosphonic acid complexes for the treatment of calcific tumors, U.S. Patent 5059412; 1991.
[7] Garlich JR, McMillan K, Masterson TT, Simon J, Wilson DA. Chemistry of novel macrocyclic aminophosphonic acid chelates of rare earth radionuclides and their in vivo biodistribution. J Nucl Med 1993;34:244P.
[8] Chakraborty S, Das T, Banerjee S, Chaudhari PR, Sarma HD, Venkatesh M, et al. Preparation and biological evaluation of Sm-153-DOTMP as a potential agent for bone pain palliation. Nucl Med Commun 2004;25:1169–76.
[9] Banerjee S, Chakraborty S, Das T, Kothari K, Samuel G, Venkatesh M, et al. Lu-177-DOTMP, Sm-153-DOTMP, Yb-175-EDTMP and Re-186/188-CTMP: novel agents for

bone pain palliation and their comparison with Sm-153-EDTMP. Founder's Day Special Issue 2005:22–37.
[10] Optimization of production and quality control of therapeutic radionuclides and radiopharmaceuticals: final report of a co-ordinated research project, 1994–1998. Vienna, Austria: International Atomic Energy Agency; 1999.
[11] Mitterhauser M, Toegel S, Wadsak W, Mien LK, Eidherr H, Kletter K, et al. Binding studies of [^{18}F]-fluoride and polyphosphonates radiolabelled with [^{99m}Tc], [^{111}In], [^{153}Sm] and [^{188}Re] on bone compartments: verification of the pre vivo model? Bone 2005;37:404–12.
[12] Beyer GJ, Offord R, Kuenzi G, Aleksandrova Y, Ravn U, Jahn S, et al. The influence of EDTMP-concentration on the biodistribution of radio-lanthanides and 225-Ac in tumor-bearing mice. Nucl Med Biol 1997;24:367–72.
[13] O'Mara RE, McAfee JG, Subramanian G. Rare earth nuclides as potential agents for skeletal imaging. J Nucl Med 1969;10:49–51.
[14] Donaldson HH. The rat: reference tables and data for the albino rat (*Mus norvegicus albinus*) and the Norway rat (*Mus norvegicus*); 1915. Philadelphia.
[15] Stabin MG, Sparks RB, Crowe E. OLINDA/EXM: the second-generation personal computer software for internal dose assessment in nuclear medicine. J Nucl Med 2005;46:1023–7.
[16] Xu XG, Eckerman KF. Handbook of anatomical models for radiation dosimetry. Boca Raton: CRC Press; 2010.
[17] Macey DJ, Williams LE, Breitz HB, Liu A, Johnson TK, Zanzonico PB. AAPM report 71: a primer for radioimmunotherapy and radionuclide therapy. Madison: Medical Physics Publishing; 2001.
[18] Breitz H. Dosimetry in a myeloablative setting. Cancer Biother Radiopharm 2002;17:119–28.
[19] Eary JF, Collins C, Stabin M, Vernon C, Petersdorf S, Baker M, et al. Samarium-153-EDTMP biodistribution and dosimetry estimation. J Nucl Med 1993;34:1031–6.